Atmos. Chem. Phys., 18, 571–586, 2018
https://doi.org/10.5194/acp-18-571-2018

Atmospheric Chemistry and Physics
Open Access
EGU

The concentration, source and deposition flux of ammonium and nitrate in atmospheric particles during dust events at a coastal site in northern China

Jianhua Qi[1], Xiaohuan Liu[1], Xiaohong Yao[1], Ruifeng Zhang[1], Xiaojing Chen[1], Xuehui Lin[2], Huiwang Gao[1], and Ruhai Liu[1]

[1]Key Laboratory of Marine Environment and Ecology, Ministry of Education,
Ocean University of China, Qingdao 266100, China
[2]Qingdao Institute of Marine Geology, China Geological Survey, Qingdao 266100, China

Correspondence: Jianhua Qi (qjianhua@ouc.edu.cn)

Received: 30 December 2016 – Discussion started: 28 February 2017
Revised: 1 December 2017 – Accepted: 6 December 2017 – Published: 18 January 2018

Abstract. Asian dust has been reported to carry anthropogenic reactive nitrogen during transport from source areas to the oceans. In this study, we attempted to characterize NH_4^+ and NO_3^- in atmospheric particles collected at a coastal site in northern China during spring dust events from 2008 to 2011. Based on the mass concentrations of NH_4^+ and NO_3^- in each total suspended particle (TSP) sample, the samples can be classified into increasing or decreasing types. In Category 1, the concentrations of NH_4^+ and NO_3^- were 20–440 % higher in dust day samples relative to samples collected immediately before or after a dust event. These concentrations decreased by 10–75 % in the dust day samples in Categories 2 and 3. Back trajectory analysis suggested that multiple factors, such as the transport distance prior to the reception site, the mixing layer depth on the transport route and the residence time across highly polluted regions, might affect the concentrations of NH_4^+ and NO_3^-. NH_4^+ in the dust day samples was likely either in the form of ammonium salts existing separately to dust aerosols or as the residual of incomplete reactions between ammonium salts and carbonate salts. NO_3^- in the dust day samples was attributed to various formation processes during the long-range transport. The positive matrix factorization (PMF) receptor model results showed that the contribution of soil dust increased from 23 to 36 % on dust days, with decreasing contributions from local anthropogenic inputs and associated secondary aerosols. The estimated deposition flux of $N_{NH_4^+ + NO_3^-}$ varied greatly from event to event; e.g., the dry deposition flux of $N_{NH_4^+ + NO_3^-}$ increased by 9–285 % in Category 1 but decreased by 46–73 % in Category 2. In Category 3, the average dry deposition fluxes of particulate nitrate and ammonium decreased by 46 % and increased by 10 %, respectively, leading to 11–48 % decrease in the fluxes of $N_{NH_4^+ + NO_3^-}$.

1 Introduction

Reactive nitrogen carried in dust particles can be transported over a long distance, and the atmospheric nitrogen deposition in oceans has been recognized as an important external source of the nitrogen supporting phytoplankton growth (Duce et al., 2008; Y. Zhang et al., 2010). This hypothesis has been evaluated through incubation experiments, in situ experiments and the use of satellite observational data (Banerjee and Kumar, 2015; Guo et al., 2012; Liu et al., 2013; Shi et al., 2012; Tan and Wang, 2014). However, the process is dynamic due to the worldwide changing emissions of NO_x and NH_3 in the last few decades. For example, China and most of the developing countries in Asia experienced a large increase in emissions of NH_3 and NO_x while a substantial decrease in emissions occurred in Europe over the last 3 decades (Grice et al., 2009; Liu et al., 2017; Ohara et al., 2007; Skjøth and Hertel, 2013). The change would affect the nitrogen carried by dust particles to some extent, and updated studies are thereby essential.

Asian dust is one of the three largest dust sources on earth. Asian dust has been reported to not only frequently cross over the mainland and the seas on the coast of China but also to occasionally reach the remote northern Pacific Ocean or North America (Creamean et al., 2013; Tan and Wang, 2014; Van Curen and Cahill, 2002; Zhang and Gao, 2007). In an extreme case, Asian dust was found to be transported more than one full circuit around the globe in approximately 13 days (Uno et al., 2009). During long-range transport, dust particles may mix with anthropogenic air pollutants and consequently undergo complicated chemical reactions (Cui et al., 2009; Li et al., 2014; Ma et al., 2012; Q. Z. Wang et al., 2011, 2016; Z. Wang et al., 2017; Xu et al., 2014; Yang et al., 2002). For example, a few studies have shown that the concentrations of atmospheric particulate NO_3^- and NH_4^+ on dust storm days were 2–5 times larger than those prior to the events in Beijing (Liu et al., 2014; Liu and Bei, 2016). Fitzgerald et al. (2015) found that almost all Asian dust events observed in South Korea contained considerable amounts of nitrate. However, W. J. Zhang et al. (2010) reported an interesting result; i.e., the concentrations of NO_3^- and NH_4^+ were lower during strong dust storm events than weak dust events. A high uncertainty appeared to exist for the amount of reactive nitrogen carried by dust particles.

A few contradictory results have also been reported in the literature, which has made scientific issues even more complicated. For example, the concentration of NO_3^- in atmospheric aerosols on dust days was significantly lower in comparison to the concentration measured immediately before or after the event at a rural site in Yulin near the Asian dust source region (Q. Z. Wang et al., 2016). The phenomenon was also observed in Shanghai, a megacity a few thousands of kilometers from dust source zones in China, and more downwind sites (Kang et al., 2013; Li et al., 2014; Wang et al., 2013).

Inorganic nitrogen reportedly contributed to $\sim 80\,\%$ of the total water-soluble nitrogen (TDN) in atmospheric particles collected over the Yellow Sea and in Qingdao (Shi et al., 2012). In the region, the dry deposition flux of the inorganic nitrogen accounted for more than 75 % for the TDN (Qi et al., 2013). When deposited to the ocean via atmospheric dry deposition, inorganic nitrogen has a great impact on marine productivity due to its bioavailability. To update and improve our knowledge on reactive nitrogen carried by dust particles, we collected atmospheric aerosol particles during and prior to (or after) the events at a coastal site adjacent to the Yellow Sea in each spring of 2008–2011. The concentrations of NO_2^-, NO_3^-, NH_4^+ and other components were determined for analysis. In this study, we focused on nitrate and ammonium by excluding nitrite because of its very low concentration. We first characterized the concentrations of NH_4^+ and NO_3^- in dust samples by comparing them with the values in atmospheric particles measured either prior to or after the event. We then conducted source apportionment to quantify their sources. Finally, we calculated and discussed the deposition flux of atmospheric particulate NH_4^+ and NO_3^- during dust events.

2 Experimental methods

2.1 Sampling

Figure 1 shows the sampling site, which is situated at the top of a coastal hill (Baguanshan) in Qingdao in northern China (36°6′ N, 120°19′ E; 77 m above sea level) and is approximately 1.0 km from the Yellow Sea to the east. A high-volume air sampler (Model KC-1000, Qingdao Laoshan Electronic Instrument Complex Co., Ltd., China) was set up on the roof of a two-story office building to collect total suspended particle (TSP) samples on quartz microfiber filters (Whatman QM-A) at a flow rate of 1 $m^3\ min^{-1}$. Prior to sampling, the filters were heated at 450 °C for 4.5 h to remove organic compounds. Our sample collection strategy involved collecting dust samples representing long-range-transported particles. We followed the definition of dust events adopted in the regulations of surface meteorological observations of China (CMA, 2004; Wang et al., 2008) and identified dust events based on the meteorological records (Weather Phenomenon) of Qingdao from the Meteorological Information Comprehensive Analysis and Process System (MICAPS) of the China Meteorological Administration. Due to no dust events lasting over 12 h (Lee et al., 2015; Su et al., 2017; Zhang et al., 2007), we collected one dust sample with a 4 h duration in a day. The sampling for dust particles started only when the measured PM_{10} mass concentration in Qingdao (http://www.qepb.gov.cn/m2/) and the forecasted dust mass over Asia (http://www-cfors.nies.go.jp/~cfors/) had greatly increased.

On 20–21 March 2010, two dust events subsequently swept across Qingdao. The online data in high time-resolution can allow two dust events to be identified accurately from the start to the end. The data confirmed that the 4 h dust samples with IDs of 20100320 and 20100321 were well separated from each other for the two events, although they may not capture the entirety of the two events. The same was true for the dust samples with IDs of 20110501 and 20110502. Table 1 lists the sampling information. Based on the forecast, we also collected aerosol particle samples immediately before (or after, but only when no sample was collected prior to dust events), which were regarded as the reference samples. These reference samples were further classified into sunny day samples and cloudy day samples. For those events missing sampling prior to dust events, we collected post-dust samples under clear and sunny weather conditions as early as possible.

Asian dust events were mostly observed in the spring at the sampling site. Our intensive samplings were concentrated in the period of March to May in 2008–2011, when a smaller outbreak for Asian dust events was observed in northern

Table 1. Sampling information for the aerosol samples collected at the Baguanshan site in the coastal region of the Yellow Sea.

Sampling year	Sample category	Sampling number	Sampling time	Weather characteristics
2008	Samples on dust days	20080301	From 13:22 to 17:22 on 1 March	Floating dust[a]
		20080315	From 13:21 to 17:21 on 15 March	Floating dust
		20080425	From 13:14 to 17:14 on 25 April	Floating dust
		20080528	From 11:38 to 15:38 on 28 May	Floating dust
		20080529	From 10:15 to 12:15 on 29 May[b]	Floating dust
	Reference samples	20080316	From 13:00 to 17:00 on 16 March	Sunny day
		20080424	From 13:00 to 17:00 on 24 April	Sunny day
		20080522	From 13:00 to 17:00 on 22 May	Cloudy day with mist
2009	Samples on dust days	20090316	From 8:25 to 12:25 on 16 March	Floating dust
	Reference samples	20090306	From 13:00 to 17:00 on 6 March	Sunny day
2010	Samples on dust days	20100315	From 11:30 to 15:30 on 16 March	Mist after floating dust
		20100320	From 10:30 to 14:30 on 20 March	Floating dust
		20100321	From 10:30 to 14:30 on 21 March	Floating dust
	Reference samples	20100324	From 11:30 to 15:30 on 24 March	Sunny day
2011	Samples on dust days	20110319	From 12:00 to 16:00 on 19 March	Floating dust
		20110415	From 12:00 to 16:00 on 15 April	Floating dust
		20110418	From 12:25 to 16:25 on 18 April	Floating dust[c]
		20110501	From 12:10 to 16:10 on 1 May	Floating dust
		20110502	From 16:00 to 20:00 on 2 May	Floating dust
	Reference samples	20110308	From 12:00 to 16:00 on 8 March	Sunny day
		20110416	From 12:00 to 16:00 on 16 April	Sunny day
		20110523	From 12:00 to 16:00 on 23 May	Sunny day

[a] Note that one dust sample 20080301 was collected on 1 March when no dust was recorded by the MICAPS. However, the MICAPS information indeed showed dust events in China on 1 March. The modeled spatial distribution of the PM_{10} mass concentration for this dust event on 1 March implies that the sample should be classified as a dust sample. The supporting figures are shown in Fig. S1.
[b] The sampling duration was reduced to only 2 h because of extremely high particle loads. In addition, the samples with IDs of 20080528 and 20080529 were subjected to two different dust events occurring over 2 days instead of continuous samples for one dust event (CMA, 2009).
[c] Note that one dust sample 20110418 was collected on 18 April when no dust was recorded by the MICAPS. However, blowing dust occurred and was recorded on 17 April by the Sand-dust Weather Almanac 2011 (CMA, 2013). The modeled spatial distribution of the PM_{10} mass concentration for this dust event on 18 April implies that the sample should be classified as a dust sample. The supporting figure is Fig. S2.

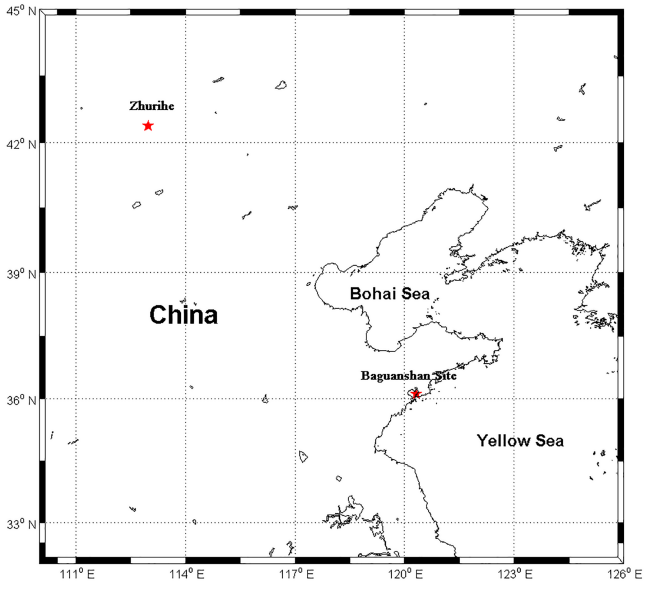

Figure 1. Location of the aerosol and dust sampling sites.

China (Fig. S3 in the Supplement). Overall, a total of 14 sets of dust samples and 8 sets of reference samples were available for analysis in this study.

To facilitate the coastal sampling data analysis, sand samples were collected at the remote site of Zhurihe (42°22′ N, 112°58′ E) in the Hunshandake Desert, one of the main Chinese sand deserts, in April 2012. Sand samples were packed in clean plastic sample bags and were stored below −20 °C before the transfer. An ice box was used to store the samples during transport to the lab for chemical analysis.

2.2 Analysis

The aerosol samples were weighted according to the standard protocol. The sample membranes were then cut into several portions for analysis. One portion of each aerosol sample was ultrasonically extracted with ultra-pure water in an ice water bath for determining inorganic water-soluble ions using ICS-3000 ion chromatography (Qi et al., 2011). The sand samples collected at the Zhurihe site were analyzed using the same procedure.

One portion of each aerosol filter was cut into 60 cm^2 pieces and digested with $HNO_3 + HClO_4 + HF$ (5 : 2 : 2 by volume) at 160 °C using an electric heating plate. The concentrations of Cu, Zn, Cr, Sc and Pb were measured using inductively coupled plasma mass spectrometry (Thermo X Series 2), while the concentrations of Al, Ca, Fe, Na and Mg were measured using inductively coupled plasma atomic emission spectroscopy (IRIS Intrepid II XSP). Field blank membranes were also analyzed for correction.

One portion of aerosol sample was digested with an HNO_3 solution (10 % HNO_3, 1.6 M) at 160 °C for 20 min in a microwave digestion system (CEM, U.S.). The Hg and As in sample extracts were analyzed following the U.S. Environmental Protection Agency method 1631E (U.S. EPA, 2002) using cold vapor atomic fluorescence spectrometry (CVAFS). The detection limits, precisions and recoveries of water-soluble ions and metal elements are listed in Table 2.

Table 2. Detection limits, precisions and recoveries of water-soluble ions and metal elements.

Component	Measurement method	Detection limit ($\mu g\,L^{-1}$)	Precision (RSD %)	Recovery (%)
NO_3^-	IC	2.72	1.54	97
SO_4^{2-}		1.62	1.55	98
NH_4^+		0.4	1.10	97
Ca^{2+}		0.44	0.79	94
Cu	ICP-MS (Xin	0.006	4.0	106
Zn	et al., 2012)	0.009	2.5	102
Cr		0.004	3.0	95
Sc		0.002	2.4	97
Pb		0.008	3.9	104
Al	ICP-AES (Lin	7.9	0.6	103
Ca	et al., 1998)	5.0	1.2	99
Fe		2.6	0.7	104
Na		3.0	0.6	99
Mg		0.6	0.6	105
Hg	CVAFS	0.0001	6.6	105
As	CVAFS	0.1	5.0	98

2.3 Computational modeling

The enrichment factor of metal elements was given by

$$\mathrm{EF}_i = \frac{(X_i/X_{\mathrm{Re}})_{\mathrm{aerosols}}}{(X_i/X_{\mathrm{Re}})_{\mathrm{crust}}}, \quad (1)$$

where subscripts i and Re refer to the studied metal and the reference metal, respectively; $(X_i/X_{\mathrm{Re}})_{\mathrm{aerosols}}$ is the concentration ratio of metal i to metal Re in the aerosol samples; and $(X_i/X_{\mathrm{Re}})_{\mathrm{crust}}$ is the ratio of metal i to metal Re in the Earth's crust. For the calculation of the enrichment factor of the metal elements, scandium was used as the reference element (Han et al., 2012), and the abundance of elements in the Earth's crust given by Taylor (1964) was adopted.

The 72 h air mass back trajectories were calculated for each TSP sample using TrajStat software (Wang et al., 2009) and National Oceanic and Atmospheric Administration (NOAA) GDAS (Global Data Assimilation System) archive data (http://www.arl.noaa.gov/ready/hysplit4.html). The air mass back trajectories were calculated at an altitude of 1500 m to identify the dust origin. In addition, the distance over sea of the air mass for each sample was measured from the trajectory using TrajStat software (Wang et al., 2009).

The positive matrix factorization (PMF) is a commonly used receptor modeling method. This model can quantify the contribution of sources to samples based on the composition or fingerprints of the sources (Paatero and Tapper, 1993; Paatero, 1997). The measured composition data can be repre-

sented by a matrix **X** of i by j dimensions, in which i number of samples and j chemical species were measured, with uncertainty u. **X** can be factorized as a source profile matrix (**F**) with the number of source factors (p) and a contribution matrix (**G**) of each source factor to each individual sample, as shown in Eq. (2).

$$\mathbf{X}_{ij} = \sum_{k=1}^{p} \mathbf{G}_{ik}\mathbf{F}_{kj} + E_{ij}, \quad (2)$$

where E_{ij} is the residual for species j of the ith sample.

The aim of the model is to minimize the objective function Q, which was calculated from the residual and uncertainty of all samples (Eq. 3), to obtain the most optimal factor contributions and profiles.

$$Q = \sum_{i=1}^{n}\sum_{j=1}^{m}\left(E_{ij}/u_{ij}\right)^2 \quad (3)$$

The EPA PMF 3.0 model was used to obtain the source apportionment of atmospheric particulates on dust and comparison days. Our modeled results satisfied the reasonable fit criteria; i.e., 90 % of the scaled residuals were located between the range −3 and +3 for each species. The correlation coefficient between the predicted and observed concentrations was 0.97.

Dry deposition velocities were obtained using Williams' model (Williams, 1982) by accounting for particle growth (Qi et al., 2005). Williams' model is a two-layer model used to calculate the dry velocity of size-segregated particles over the water. In an upper layer below a reference height (10 m), the deposition of aerosol particles is governed by turbulent transfer and gravitational settling. In the deposition layer, the gravitational settling of particles is affected by particle growth due to high relative humidity. To obtain the deposition velocity of different particle sizes, Williams' model needs many input parameters, such as the wind speed at 10 m height (U_{10}), air and water temperature and relative humidity. Relative humidity, air temperature and U_{10} from the National Centers for Environmental Prediction (NCEP) were used in this study. Surface seawater temperature data were collected from the European Centre for Medium-Range Weather Forecasts (ECMWF). The meteorological and seawater temperature data had a 6 h resolution. According to a previously reported method (Qi et al., 2013), the dry deposition fluxes of the particles and the nitrogen species were calculated for dust and comparison days.

The CMAQ model (v5.0.2) was applied over the East Asia area to simulate the concentrations of PM_{10}, NO_x and NH_3 for 14 dust samples. The simulated domain contains 164×97 grid cells with a 36 km spatial resolution, and the centered point was 110° E, 34° N. The vertical resolution includes 14 layers from the surface to the tropopause, with the first model layer at a height of 36 m above ground level. The meteorological fields were generated by the Weather Research and Forecasting (WRF) Model (v3.7). Considering that the simulated area is connected to the Yellow Sea, the CB05Cl chemical mechanism was chosen to simulate the gas-phase chemistry. Zhang et al. (2009) generated the emissions of air pollutants in 2006 including NO_x and NH_3 over East Asia and they updated the emission inventory in 2008, which we have used in this study. Initial conditions (ICONs) and boundary conditions were generated from a global chemistry model of GEOS-CHEM. All the dust events simulations are performed separately, each with a 1-week spin-up period to minimize the influence of the ICONs. The validation of the application of the CMAQ model in China has been reported by Liu et al. (2010a, b).

2.4 Other data sources and statistical analysis

Meteorological data were obtained from the Qingdao Meteorological Administration (http://qdqx.qingdao.gov.cn/zdz/ystj.aspx) and the MICAPS of the Meteorological Administration of China. Different weather characteristics, such as sunny days, cloudy days and dust days, were defined according to information from the MICAPS and Qingdao Meteorological Administration. According to the altitude, longitude and latitude of the 72 h air mass back trajectory of each dust sample, the pressure level, temperature and relative humidity (RH) data along the path of the air mass were derived from the NCEP/NCAR reanalysis system (http://www.esrl.noaa.gov/psd/data/gridded/data.ncep.reanalysis.html) for each sample. The mixed layer depth during the air mass transport of dust samples was obtained from the HYSPLIT Trajectory Model (http://ready.arl.noaa.gov/hypub-bin/trajasrc.pl) using the same method. Then the average mixing layer, transport altitude, air temperature and RH were calculated as an average of all points on the air mass back trajectory of each sample. Spearman correlation analysis was applied to examine the relationships of nitrate and ammonium with transport parameters, and P values of < 0.05 were considered to be statistically significant.

3 Results

3.1 Characterization of aerosol samples collected during dust events

We first examined the mass concentrations of TSP samples and the concentrations of crustal and anthropogenic metals therein through a comparison with the samples collected on dust days and reference samples immediately before or after dust days, providing the background information for our target species analyzed later. The comparative results are highlighted below. For these reference samples, the TSP mass concentrations ranged from 94 to 275 $\mu g\,m^{-3}$, with an average of 201 $\mu g\,m^{-3}$ (Fig. 2, Table S1). The TSP mass concentration increased substantially to 410–3857 $\mu g\,m^{-3}$ in dust day samples, with an average of 1140 $\mu g\,m^{-3}$. In each in-

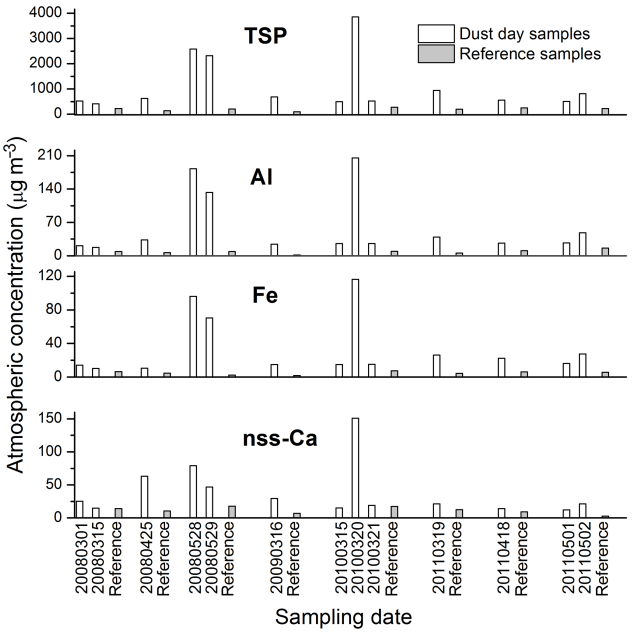

Figure 2. Mass concentrations of TSP, Al, Fe and nss-Ca in aerosol samples collected at the Baguanshan site on dust and reference days during March–May from 2008 to 2011.

dividual pair of a dust day sample and a reference sample, a net increase in the mass concentration of TSPs was observed. The percentages varied from 82 to 1303 % for dust samples compared to references, with a mean value of 403 % (Table S1). A similar increase was present in the crustal elements in each pair of samples. For example, the mean concentrations of Sc, Al, Fe, Mg and nss-Ca (usually used as a typical dust index) increased by more than a factor of 2. On the other hand, the enrichment factors (EF) of Al, Fe, Ca and Mg were less than three in dust day samples with values less than 14 in the reference samples (Table 3). Lower values are indicative of elements from a primarily crustal origin. The average mass concentrations of anthropogenic elements, such as Cu, Pb, Zn, Cr, Hg and As, in dust day samples increased by 107 to 722 % compared to those in the reference sample; however, the EF of the anthropogenic metal elements decreased in the former. This indicates that dust particles likely carried more anthropogenic elements, although their relative contribution to the total mass was lower than that in the reference sample. Note that Sample 20110415 was excluded for further analysis. It was judged as a local blowing dust event because no corresponding dust event existed upwind.

3.2 Concentrations of NH_4^+ and NO_3^- in dust day samples

When the mass concentrations of NH_4^+ and NO_3^- in each pair of TSP samples were compared, the concentrations of NH_4^+ increased by 8–473 % in some dust day samples (20080301, 20080315, 20090316, 20100315, 20100320, 20100321, 20110418 and 20110502), but decreased by 28–84 % in other dust day samples (Fig. 3, Column NH_4^+ and NO_3^- in Table S1). The same was generally true for the measured concentrations of NO_3^-.

Considering the relative values of NH_4^+ and NO_3^- in dust day samples relative to the reference samples, we classified

Table 3. The average concentrations and EFs of metal elements on dust and non-dust days.

Element	Concentration (ng m^{-3})		EF*	
	Reference days	Dust days	Reference days	Dust days
Sc	1.11	13.90	–	–
Al	8.53×10^3	6.86×10^4	3.8	1.4
Fe	4.91×10^3	3.88×10^4	3.	1.2
Ca	1.05×10^4	4.29×10^4	14.0	2.1
Mg	1.62×10^3	1.58×10^4	3.5	1.1
Cu	50.2	124.5	36.3	6.1
Pb	127.9	221.0	389.4	56.1
Zn	340.0	457.7	248.9	20.6
Cr	33.8	244.0	44.0	11.1
Hg	0.26	0.36	176.0	13.8
As	25.5	27.4	707.2	43.9

* EF values less than 10 indicate that the studied element is mainly derived from crustal sources, whereas EF values much higher than 10 indicate an anthropogenic source.

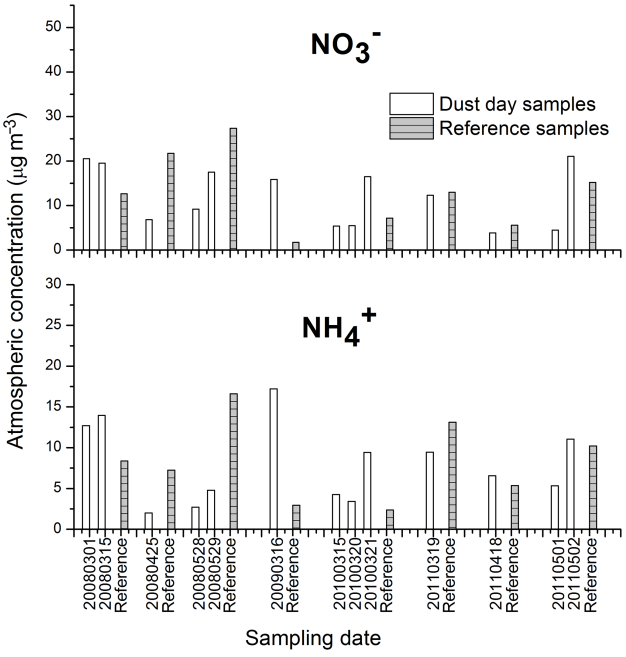

Figure 3. Mass concentrations of NH_4^+ and NO_3^- in aerosol samples collected at the Baguanshan site on dust and reference days during March–May from 2008 to 2011.

Table 4. Average measured concentrations of NH_4^+, NO_3^-, TSP, NO_x, relative humidity (RH) and air temperature for each aerosol sample category in Qingdao.

	Sample number	TSP ($\mu g\,m^{-3}$)	NO_3^- ($\mu g\,m^{-3}$)	NH_4^+ ($\mu g\,m^{-3}$)	RH (%)	T (°C)	NO_x ($\mu g\,m^{-3}$)	Summary
Category 1	20080301	527	20.5	12.7	57	7.0	36	NH_4^+ and NO_3^- concentration in dust day samples higher than reference samples
	20080315	410	19. 5	29.9	62	11.0	59	
	20090316	688	15.9	17.2	27	16.0	75	
	20100321	519	16.5	9.4	51	8.8	76	
	20110502	810	21.0	11.0	49	17.7	62	
Category 2	20080425	622	6.8	2.0	30	18.0	40	NH_4^+ and NO_3^- concentration in dust day samples lower than reference samples
	20080528	2579	9.2	2.7	17	27.0	34	
	20080529	2314	17.5	4.8	60	20.0	29	
	20110319	939	12.3	9.4	16	12.6	93	
	20110501	502	4.5	5.3	23	21.6	66	
Category 3	20100315	501	5.4	4.3	30	7.2	73	NO_3^- concentration in dust day samples lower than reference samples; NH_4^+ close to reference samples
	20100320	3857	5.5	3.4	35	10.6	92	
	20110418	558	3.8	6.6	33	12.6	47	
Reference samples*	20080316	225	12.6	8.4	28	11.0	60	
	20080424	137	21.7	7.2	49	18.0	53	
	20080522	206	27.4	16.6	78	20.0	60	
	20090306	94	2.9	3.0	29	7.00	51	
	20100324	275	7.2	2.4	23	9.0	82	
	20110308	194	13.0	13.1	20	11.5	111	
	20110416	252	5.6	5.4	26	14.1	55	
	20110523	224	15.2	10.2	42	20.6	49	

* For the corresponding reference sample for each dust event, see Table 1.

the dust day samples into three categories (Table 4). In Category 1, the mass concentrations of NH_4^+ and NO_3^- were larger in dust day samples compared to the reference samples. In Category 2, the reverse was true. In Category 3, the mass concentrations of NO_3^- were lower in the dust samples than in the reference samples, whereas the concentrations of NH_4^+ were close to the reference. As reported, the Yellow Sea encountered dust storms mainly derived from the Hunshandake Desert (Zhang and Gao, 2007). We thereby compared our observations with the sand particles collected from this desert (Table 5). The ratios of mass concentrations of nitrate and ammonium to the total mass of sand particles were very low, i.e., less than $81\,\mu g\,g^{-1}$, which are approximately 3 orders of magnitude less than the corresponding values in our dust samples. The values obtained from atmospheric aerosols at the urban sites of Duolun (Cui, 2009) and Alxa Right Banner (Niu and Zhang, 2000), which are closer to the desert, increased on dust days, but were still over 1 order of magnitude lower than the corresponding values in this study (Table 5). The mixing and chemical interaction between anthropogenic air pollutants and dust particles during transport from the source zone to the reception site likely played an important role in increasing the ratios, leading to extremely larger ratio values at this site relative to those in source dust and in upwind atmospheric particles (Cui et al., 2009; Wang et al., 2011; Wu et al., 2017). Since air pollutant emissions, meteorological conditions, chemical reactions and others can affect the concentrations of NH_4^+ and NO_3^- in atmospheric particles collected on dust days, the observed increase or decrease in the mass concentration of nitrate and ammonium in different dust samples compared to the reference implied the combined effect of those factors.

4 Discussion

4.1 Theoretical analysis of the three categories

Ammonium salts are common in atmospheric particles with diameters of less than 2 µm (Yao et al., 2003; Yao and Zhang, 2012). Many modeling studies have shown that the gas–aerosol thermodynamic equilibrium is assumed to be fully attained for inorganic ions, including ammonium salts in $PM_{2.5}$ (Dentener et al., 1996; Underwood et al., 2001; Z. Wang et al., 2017; Zhang et al., 1994; Zhang and Carmichael, 1999). Reasonably good agreements between ammonium salt modeling results and observations reported in the literature support the validity of this assumption (Chen et al., 2016; Penrod et al., 2014; Walker

Table 5. Comparison of the NH_4^+ and NO_3^- content in sand and aerosol particles on dust days or close to the dust source region (unit: $\mu g\,g^{-1}$).

Sands sampled in dust source regions			Aerosols in or close to dust source region on dust days			Aerosols in the coastal region of the Yellow Sea	
Study region and data source	Relative concentration[a]		Study region and data source	Relative concentration[a]			
	NO_3^-	NH_4^+		NO_3^-	NH_4^+	NO_3^-	NH_4^+
Zhurihe (this study)	25.46 ± 22.87	4.21 ± 1.03	Duolun (Cui, 2009)	1200	900	Reference samples: $28\,200 \pm 24\,819$	Reference samples: $24\,063 \pm 21\,515$
Alxa Left Banner, Inner Mongolia (Niu and Zhang, 2000)	62.1 ± 7.4	79.1 ± 1.1	Alxa Right Banner, Inner Mongolia (Niu and Zhang, 2000)	1975[b]	4091[b]	Category 1: $34\,892 \pm 9570$	Category 1: $22\,571 \pm 7016$
Yanchi, Ningxia (Niu and Zhang, 2000)	46.4 ± 2.2	80.9 ± 1.3	Hinterland of the Taklimakan Desert, Xinjiang (Dai, 2016)	142–233	2–15	Category 2: 5542 ± 5117	Category 2: 4758 ± 5698
			Average of Sonid Youqi, Huade (Inner Mongolia), Zhangbei (Hebei) (Mori et al., 2003)	253	710	Category 3: 6359 ± 4697	Category 3: 7059 ± 5591
			Yulin, the north edge of Loess Plateau (Wang et al., 2011)	216.4	80.6		
			Golmud, Qinghai (Sheng et al., 2016)	892.9	–[c]		
			Hohhot, Inner Mongolia (Yang et al., 1995)	588.1	No data		

[a] Relative concentration of NH_4^+ and NO_3^- per aerosol particle mass.
[b] Samples collected on a floating dust day (horizontal visibility less than 10 000 m and very low wind speed).
[c] The ammonium concentration was lower than the detection limit of the analytical instrument.

et al., 2012). Supposing that a thermodynamic equilibrium had been attained by the ammonium salts in Category 1, the reactions between carbonate salts and ammonium salts, such as (1) $(NH_4)_2SO_4 + CaCO_3 \Rightarrow CaSO_4 + NH_3\,(gas) + CO_2\,(gas) + H_2O$ and (2) $2NH_4NO_3 + CaCO_3 \Rightarrow Ca(NO_3)_2 + 2NH_3\,(gas) + CO_2\,(gas) + H_2O$, will release NH_3 (gas) until $CaCO_3$ has been completely used up. During dust events, very high concentrations of Ca^{2+} were observed, and high $CaCO_3$ concentrations were therefore expected. For example, the single-particle characterization showed that Asia dust from the Gobi and Inner Mongolian deserts had rich $CaCO_3$, with a ratio of 4.3–6.7 % for reacted $CaCO_3$ and 3.0–4.6 % for unreacted $CaCO_3$ (Hwang et al., 2008). Heterogeneous chemical reactions of mineral dust mostly occurred on $CaCO_3$ mineral dust (Hwang and Ro, 2006). However, when Category 1 was considered alone except for Sample 20100321, a good correlation was obtained for $[NH_4^+]_{\text{equivalent concentration}} = 0.98 \times [NO_3^- + SO_4^{2-}]_{\text{equivalent concentration}}$ ($R^2 = 0.83$, $P < 0.05$). The good correlation, together with the slope of 1, strongly indicated that the NO_3^- and SO_4^{2-} were almost completely associated with NH_4^+ in these dust day samples. Anthropogenic ammonium nitrate and ammonium sulfate were thought to be produced by gas, aqueous-phase reactions and thermodynamic equilibrium processes, and they were usually internally mixed (Seinfeld and Pandis, 1998). Conversely, the poor correlation of Ca^{2+} to NO_3^- and SO_4^{2-} showed that the formation of $CaSO_4$ and/or $Ca(NO_3)_2$ was probably negligible. Thus, ammonium salt aerosols very likely existed separately to dust aerosols in these dust day samples. Z. Wang et al. (2017) also found that coarse-mode ammonium was quite low and fine-mode dust particles existed separately to anthropogenic ammonium nitrate and ammonium sulfate. The observed NO_3^- and NH_4^+ in Asia dust samples were argued to be due to the physical mixing of two types of particles rather than the heterogeneous formation of nitrate and ammonium (Huang et al., 2010). The hypothesis appeared to be valid in Category 1, where NH_4^+ was negatively correlated with Ca^{2+} (Fig. S4). In Sample 20100321 collected on 21 March 2010, $[NH_4^+]$ only

accounted for ∼ 70 % of the observed $[NO_3^- + SO_4^{2-}]$ in an equivalent concentration. This result suggested that ∼ 30 % of $(NO_3^- + SO_4^{2-})$ may be associated with dust aerosols via the formation of metal salts of the two species. This hypothesis was supported by the correlation result; i.e., NO_3^- was positively correlated with NH_4^+ and Cu, and SO_4^{2-} was correlated with K^+, Na^+ and Mg^{2+} (Fig. S4). Scheinhardt et al. (2013) found that Cu^{2+} showed mixed organic and nitrate complexation in aerosol particles, using a thermodynamic model (E-AIM III). Cu was also detected to be partly in the form of nitrate in aerosol particles by single-particle mass spectrometry (H. Wang et al., 2016; Zhang et al., 2015). Cu was once used as an effective marker of diesel and biodiesel-blend exhaust (Gangwar et al., 2012), while it can also be derived from copper pyrites ($CuFeS_2$) in Inner Mongolia mines (Huang et al., 2010). The increase of Cu in the mass concentration in dust samples implied dust particles mixed with anthropogenic particles, particularly from industrial emissions, during transport. In addition, many studies showed that SO_4^{2-} can exist in many forms of metal salts in atmospheric particles, such as Na_2SO_4, K_2SO_4, $K_2Ca(SO_4)_2 \cdot H_2O$, $Na_2Ca(SO_4)_2$, $Na_2Mg(SO_4)_2 \cdot 4H_2O$, $(NH_4)_2Mg(SO_4)_2 \cdot 6H_2O$, and $Na_3(NO_3)(SO_4) \cdot H_2O$ (Chabas and Lefèvre, 2000; Sobanska et al., 2012; Xie et al., 2005).

For Category 2, no correlation between $[NH_4^+]_{\text{equivalent concentration}}$ and $[NO_3^- + SO_4^{2-}]_{\text{equivalent concentration}}$ existed. When Category 2 was considered alone except for one Sample 20110501, the equivalent ratios of NH_4^+ to $NO_3^- + SO_4^{2-}$ were generally much smaller than 1, suggesting that a larger fraction of $NO_3^- + SO_4^{2-}$ may exist as metal salts due to reactions of their precursors with dust aerosols. NO_3^- and SO_4^{2-} showed no correlation with NH_4^+ but did show significant correlation with Pb (Fig. S4). The average concentration of Ca^{2+} in Category 2 ($0.43 \pm 0.40\,\mu mol\,m^{-3}$) was evidently higher than that in Category 1 (Ca^{2+}: $0.17 \pm 0.04\,\mu mol\,m^{-3}$), implying the probable formation of $CaSO_4$ and/or $Ca(NO_3)_2$ and the release of NH_3 (gas). Moreover, except for 20080502, the remaining dust samples in Category 2 were transported from the desert relatively enriched with $CaCO_3$ (1–25 % in wt %) (Formenti et al., 2011). A positive correlation between NO_3^- and SO_4^{2-} in Category 2 compared to a negative correlation in Category 1 also implied that the dust particles enriched with $CaCO_3$ in Category 2 might play an important role to form SO_4^{2-} and NO_3^-. Ca-rich dust particles coated with highly soluble nitrate were observed at Kanazawa in Japan during Asian dust storm periods using SEM/EDX (scanning electron microscopy equipped with an energy dispersive X-ray spectrometer) (Tobo et al., 2010). The single-particle observation conducted by Hwang and Ro (2006) showed that $CaCO_3$ in dust particles was almost completely consumed to produce mainly $Ca(NO_3)_2$ species.

There were only three samples in Category 3. $[NH_4^+]_{\text{equivalent concentration}} = 0.95 \times [NO_3^- + SO_4^{2-} + Cl^-]_{\text{equivalent concentration}}$ was obtained for Sample 20110418, implying that the NH_4^+ was not only associated with NO_3^- and SO_4^{2-} but also with Cl^-. In the sample collected on 15 March 2010, $[NH_4^+]$ accounted for 78 % of the observed $[NO_3^- + SO_4^{2-}]$ in an equivalent concentration. As discussed above, ∼ 20 % of $(NO_3^- + SO_4^{2-})$ may be associated with dust aerosols via the formation of metal salts of the two species. The equivalent ratio of NH_4^+ to $NO_3^- + SO_4^{2-}$ was only 0.14 for Sample 20100320, and Ca^{2+} for this sample ($0.47\,\mu mol\,m^{-3}$) was evidently higher than that for Sample 20100315 (Ca^{2+}: $0.12\,\mu mol\,m^{-3}$) and 20110418 (Ca^{2+}: $0.12\,\mu mol\,m^{-3}$), suggesting that a larger fraction of $NO_3^- + SO_4^{2-}$ may exist as metal salts. However, the unique changes in NH_4^+ and NO_3^-, different from Category 1 and 2, need further investigation.

4.2 Source apportionment of aerosols during dust and non-dust events

The sources of atmospheric aerosols in dust and reference samples were determined by PMF modeling (Paatero and Tapper, 1993; Paatero, 1997). Figure 4 shows that atmospheric aerosols in the reference samples mainly included six sources, i.e., industry, soil dust, secondary aerosols, sea salt, biomass burning and coal combustion/other sources. In these dust samples, including Categories 1–3, oil combustion, industry, soil dust, secondary aerosols and coal combustion/other sources were identified as five major sources (Table 6). The contribution of soil dust evidently increased from 23 to 36 % in the dust samples relative to the reference, consistent with the high concentrations of TSPs and crustal metals observed on dust days. The calculated contribution of nitrate plus ammonium from the soil dust source to the total mass of nitrate plus ammonium in the dust samples greatly increased. The source profile for coal combustion in the dust day samples showed a high percentage of K^+, Cl^-, Ca, Mg, Co, Ni, As, Al and Fe, indicating that coal combustion particles may exist contemporaneously with other anthropogenic pollutants emitted along the transport path. Liu et al. (2014) also found a larger net increase in the contribution of dust aerosols to the mass of PM_{10}, i.e., 31–40 %, on dust days compared to non-dust days in Beijing, which is approximately 600 km upwind of Qingdao. Accordingly, they reported that the contributions of local anthropogenic sources decreased on dust days, especially those from secondary aerosols, consistent with the EF of anthropogenic metals observed on dust days.

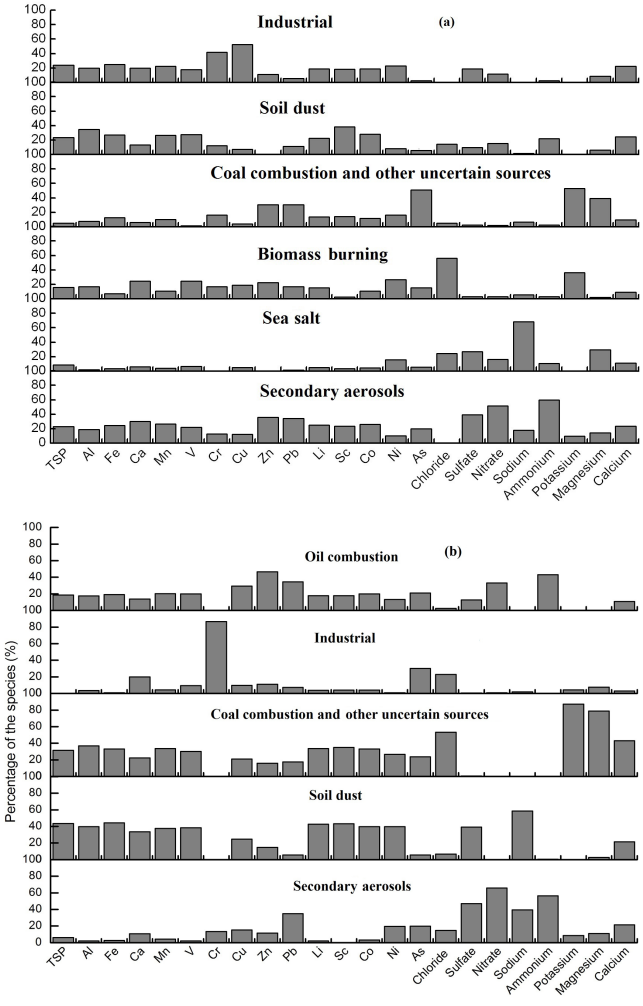

Figure 4. Source profiles of atmospheric aerosol samples collected on reference **(a)** and dust **(b)** days using the PMF model.

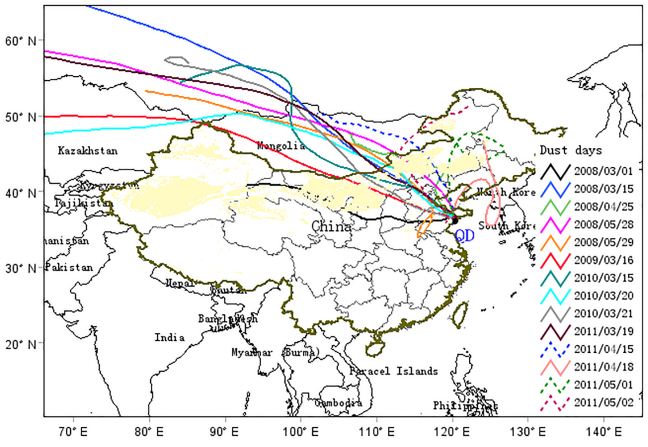

Figure 5. The 72 h backward trajectories for dust samples from 2008 to 2011 (the yellow domains in the map represent the dust source regions in China).

Table 6. Sources and source contributions (expressed in %) calculated for aerosol samples collected during dust and non-dust events.

Dust event		Reference days	
Source	% of TSP	Source	% of TSP
Soil dust	36	Soil dust	23
Industrial	21	Industrial	24
Secondary aerosol	6	Secondary aerosol	23
Oil combustion	6	Biomass burning	16
Coal combustion and other uncertain sources	31	Coal combustion	5
		Sea salt	9

4.3 Influence of transport pathways on NH_4^+ and NO_3^- in dust samples

The calculated air mass trajectories for 13 out of 14 samples showed that the air mass originated from Inner Mongolia, northern China (Fig. 5), generally consistent with the results of Zhang and Gao (2007). The remaining one, with an ID of 20110418 originated from Northeast China. The calculated trajectories showed that the entire dust air mass passed over these highly polluted regions with strong modeled emissions of NO_x and NH_3, shown in Fig. 6, and experienced different residence times in these regions. Figure 5 shows that all air mass trajectories in Category 1 were transported from either the north or northwest over the continent, except for Sample 20110502. In Category 2, the air masses always traveled 94–255 km over the sea prior to arriving at the reception site. NH_3-poor conditions in the marine atmosphere disfavored the formation and existence of ammonium nitrate. On the other hand, the humid marine conditions (the calculated average RH ranged from 50 to 75 % over the Bohai and Yellow seas in 2006–2012 using NCEP/NCAR reanalysis data) might have enhanced hetero-coagulation between dust and smaller anthropogenic particles, leading to the release of NH_3 via reactions between preexisting ammonium salts and carbonate salts.

The average mixing layer was less than 900 m along the air mass transport routes for most sampling days in Category 1 (Table 7), favoring the trapping of locally emitted anthropogenic air pollutants in the mixing layer. The air masses in Category 1 took over 11–39 h to cross over the highly polluted area with appreciable modeled concentrations of NO_x (5.7 ± 1.4 ppb) and NH_3 (7.6 ± 3.3 ppb). Except for two samples (IDs of 20080529 and 20110319), air masses in Category 2 took less than 10 h to cross over the polluted areas, with lower concentrations of NO_x (modeled value:

Table 7. Concentrations of TSP, NO_3^- and NH_4^+; transport speed; transport distance over the sea; transport distance; air temperature; RH; average mixed layer during transport and transport time in polluted regions for atmospheric aerosol samples on dust days.

Group	Sample number	TSP ($\mu g\,m^{-3}$)	NO_3^- ($\mu g\,g^{-1}$)	NH_4^+ ($\mu g\,g^{-1}$)	Speed ($km\,h^{-1}$)	Distance over the sea (km)	Transport altitude (m)	Mixed layer depth (m)	R-time[a] (h)	T[b] (°C)	RH[c] (%)
Category 1	080301	527	38 984	24 107	40.1	0	1160 ± 702	864 ± 745	39	-2.9 ± 11.7	29 ± 10
$NH_4^+ > RS^d$	080315	410	47 611	34 130	79.1	0	4921 ± 1870	950 ± 525	13	-32.5 ± 16.4	34 ± 16
$NO_3^- > RS^d$	090316	688	23 050	25 012	86.2	0	3739 ± 1083	702 ± 665	11	-19.1 ± 11.7	42 ± 17
	100321	519	31 741	18 155	87.2	0	3407 ± 1249	1113 ± 760	19	-23.0 ± 13.6	42 ± 22
	110502	810	25 995	13 632	30.2	177	3666 ± 1371	747 ± 957	26	-13.2 ± 15.8	31 ± 13
Category 2	080425	256	4089	372	29.6	0	887 ± 656	1161 ± 1040	10	-2.7 ± 6.1	66 ± 13
$NH_4^+ < RS^d$	080528	2579	232	72	88.2	244	4336 ± 1461	1064 ± 830	8	-15.5 ± 13.6	31 ± 16
$NO_3^- < RS^d$	080529	2314	26	166	63.7	94	2148 ± 1725	1194 ± 816	43	3.6 ± 18.4	25 ± 17
	110319	939	13 088	10 067	70.6	132	4271 ± 1867	790 ± 719	27	-26.3 ± 20.0	48 ± 32
	110501	502	8924	10 631	35.1	252	3212 ± 810	916 ± 1114	5	-13.4 ± 8.5	39 ± 13
Category 3	100315	501	10 767	8515	57.3	0	5009 ± 1410	1110 ± 365	7	-40.4 ± 13.3	45 ± 29
$NO_3^- < RS^d$	100320	3857	1418	884	76.9	0	1284 ± 401	525 ± 371	10	-12.2 ± 6.3	61 ± 16
$NH_4^+ \cong RS^d$	110418	558	6891	11 778	35.6	931	1344 ± 780	695 ± 672	2	-0.1 ± 8.2	52 ± 28

[a] Residence time of the air mass passing over parts of highly polluted regions according to the trajectories of samples.
[b] Average air temperature; the definition is given in Sect. 2.4.
[c] Average relative humidity; the definition is given in Sect. 2.4.
[d] Reference samples.

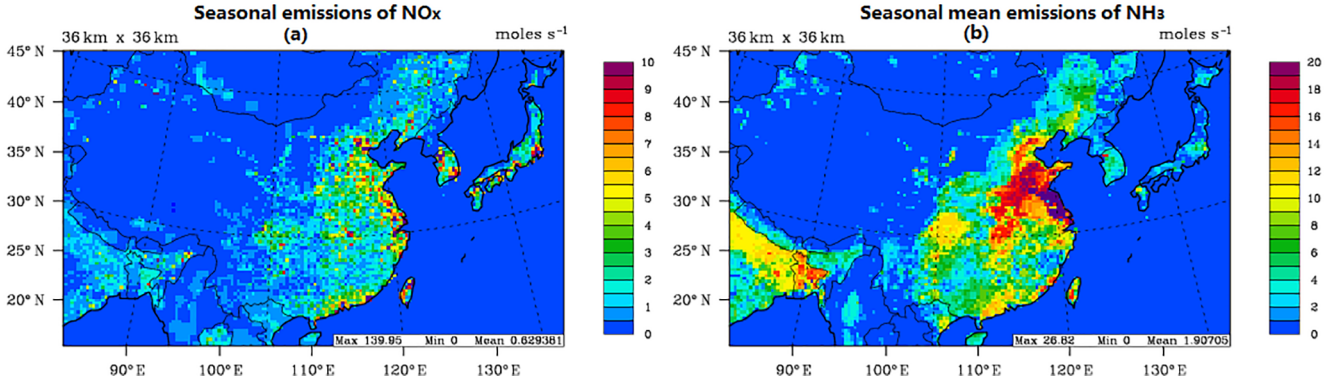

Figure 6. Seasonal mean emissions of NO_x **(a)** and NH_3 **(b)** over East Asia during March–May 2008.

3.6 ± 3.4 ppb) and NH_3 (modeled value: 4.7 ± 4.7 ppb), and the mixing layer height along the route was 916–1194 m (on average) for each dust event. Moreover, the averaged wind speed at sampling site was $2.8\,m\,s^{-1}$ in Category 1, but $6.2\,m\,s^{-1}$ in Category 2. The lower wind speed in Category 1 was unexpected, implying dust particles very likely traveled aloft at a high speed and then mixed down to the ground through subsidence. This further led to the external mixing of anthropogenic particulate matter and dust. The correlation analysis results in Table S2 indirectly support these conclusions.

The concentrations of PM_{10} and its major components NO_3^- and NH_4^+ over East Asia on dust days and comparison days were modeled using the WRF-CMAQ model (Fig. S5–S6). Spatial distributions of simulated PM_{10} during each dust events were consistent with the records in the Sand-dust Weather Almanac (CMA, 2009, 2010, 2012, 2013). The dust particles were transported eastward by passing over the sampling site, the East China Sea, and arriving at the far remote ocean region, except for the local blowing dust sample with an ID of 20110415, as mentioned previously. NMB (normalized mean bias) values of simulated NO_3^- were -4 and -12 % in dust and non-dust reference samples, respectively, indicating that CMAQ results reasonably reproduce the mass concentrations of NO_3^- (Fig. S6). Simulated NH_4^+ concentrations in dust samples were severely underpredicted, with NMB values of -71 %. For reference samples, simulated NH_4^+ concentrations sometimes can well reproduce the observational values, but the simulation was sometimes severely deviated from the observation. The deviation could be related to many factors which were outside of the scope of this study. The separate mixing mechanism proposed in this study urgently needs to be included in the model for accurately predicting concentrations during dust events.

Table 8. Dry deposition of TSP (mg m^{-2} month^{-1}), $N_{NH_4^+ + NO_3^-}$ (mg N m^{-2} month^{-1}) and some trace metals (mg m^{-2} month^{-1}) on dust and reference days.

	Dry deposition flux							
	TSP	NO_3^- -N	NH_4^+-N	$N_{NH_4^+ + NO_3^-}$	Fe	Cu	Pb	Zn
Category 1*	8000 ± 1800	65 ± 9	24 ± 14	90 ± 17	533 ± 179	2 ± 0.3	0.3 ± 0.3	6 ± 2
Category 2*	$18\,000 \pm 11\,000$	13 ± 18	8 ± 4	21 ± 22	1300 ± 1000	3 ± 2	0.08 ± 0.04	4 ± 1
Category 3*	$29\,000 \pm 31\,000$	26 ± 6	17 ± 8	42 ± 12	2100 ± 2200	6 ± 1	0.20 ± 0.02	5 ± 3
Reference samples	2800 ± 700	48 ± 33	15 ± 8	63 ± 39	190 ± 110	1 ± 1	0.09 ± 0.1	5 ± 4

*For the characterization of $N_{NH_4^+ + NO_3^-}$ concentration and sample information of the category, see Table 3.

4.4 Dry deposition fluxes of TSP, NH_4^+, NO_3^- and metals

Dust events are known to increase the deposition fluxes of aerosol particles along the transport path because of high particle loadings. For example, Fu et al. (2014) found that the long-range transported dust particles increased the dry deposition of PM_{10} in the Yangtze River Delta region by a factor of approximately 20. In terms of atmospheric deposition in the oceans, a few studies reported enhancements in oceanic chlorophyll *a* following dust storm events (Banerjee and Kumar, 2015; Tan and Wang, 2014). In addition to that in high-nutrient and low-chlorophyll (HNLC) regions, the input of nitrogen and other nutrients associated with dust deposition is expected to promote the growth of phytoplankton in oceans with varying nutrient limitation conditions. Thus, we calculated the dry deposition fluxes of aerosols particles, $N_{NH_4^+ + NO_3^-}$ and metal elements during dust and reference periods using the measured component concentrations and modeled dry deposition velocities (Table 8). We also compared the calculated dry deposition flux of TSP and $N_{NH_4^+ + NO_3^-}$ with previous observations in the literature.

The calculated dry deposition fluxes of atmospheric particulates increased on dust days compared to the reference to some extent. For example, the particle deposition fluxes varied over a wide range from 5200 to 65 000 mg m^{-2} month^{-1} on different dust sampling days, with an average of 18 453 mg m^{-2} month^{-1}, in comparison with the dry deposition flux of TSP of 2800 ± 700 mg m^{-2} month^{-1} from the reference periods in the coastal region of the Yellow Sea. The dry deposition fluxes of $N_{NH_4^+ + NO_3^-}$ varied, depending on Category 1, 2 or 3. In Category 1, the dry deposition fluxes of $N_{NH_4^+ + NO_3^-}$ increased by 9–75 % with increased TSP flux by 86–252 % (Table S3). In Categories 2 and 3, the dry deposition fluxes of TSP increased by 126 to 2226 % compared to the reference. The dry deposition fluxes of particulate $N_{NH_4^+ + NO_3^-}$ decreased by 50 %, on average, in Categories 2 and 3, although the fluxes of ammonium of two samples in Category 3 increased. A larger decrease compared to the reference in the flux of nitrate was present in Categories 2 and 3, i.e., decreases of 73 and 46 %, respectively. The ammonium deposition flux also decreased by 47 % in Category 2 but increased by 10 % in Category 3.

Except for Pb and Zn in Category 2, the calculated dry deposition fluxes of Cu, Pb and Zn increased with those of nitrogen on dust days. Trace metals were found to have a toxic effect on marine phytoplankton and inhibit their growth (Bielmyer et al., 2006; Echeveste et al., 2012). Liu et al. (2013) found that inhibition coexisted with the promotion of phytoplankton species in incubation experiments in the southern Yellow Sea in the spring of 2011 by adding Asian dust samples to collected seawater. However, the calculated dry atmospheric deposition fluxes of Fe increased by a factor of 124–2370 % in dust day samples. F. J. Wang et al. (2017) recently reported that Fe can alleviate the toxicity of heavy metals. Moreover, atmospheric inputs of iron to the ocean have been widely proposed to enhance primary production in HNLC areas (Jickells et al., 2005).

Due to anthropogenic activity and economic development, NO_x and NH_3 emissions were reported to increase in China from 1980 to 2010 (Fig. S3; Liu et al., 2017). The dry deposition flux of $N_{NH_4^+ + NO_3^-}$ should have theoretically increased with the increase in the emission of inorganic nitrogen. Considering the different dry deposition velocities to be used in various studies, we recalculated the dry deposition flux of $N_{NH_4^+ + NO_3^-}$ in the literature using the dry deposition velocities of 1 cm s^{-1} for nitrate and 0.1 m s^{-1} for ammonium, as reported by Duce et al. (1991). We thereby found that dry deposition fluxes of $N_{NH_4^+ + NO_3^-}$ over the Yellow Sea during the dust days increased greatly from 1999 to 2007, but the values in Qingdao varied narrowly within a range of 94.75–99.65 mg N m^{-2} month^{-1} during the dust days from 1997 to 2011 (Table 9). The complicated results implied that even more updated works are needed in the future.

5 Conclusion

The concentrations of nitrate and ammonium in TSP samples varied greatly from event to event on dust days. Relative to the reference samples, the concentrations were both higher

Table 9. Comparison of dry deposition flux and normalized flux of TSP (mg m^{-2} month^{-1}) and $N_{NH_4^+ + NO_3^-}$ (mg N m^{-2} month^{-1}) with observations from other studies (mg N m^{-2} month^{-1}).

Source	Year	Area		TSP	$N_{NH_4^+ + NO_3^-}$	Normalized average flux of $N^*_{NH_4^+ + NO_3^-}$
This work	2008–2011	Qingdao, coastal region of the Yellow Sea	Reference day	2800 ± 700	63 ± 39	93.90
			Dust day	$10\,138 \pm 15\,940$	58 ± 36	101.39
			Average of dust and reference			97.64
Qi et al. (2013)	2005–2006	Qingdao, coastal region of the Yellow Sea	Average of nine months samples	159.2–3172.9	1.8–24.5	94.75
Zhang et al. (2011)	1997–2005	Qingdao	Average of annual samples		132	99.65
Zhang et al. (2007)	1999—2003	The Yellow Sea			11.43	9.91
Shi et al. (2013)	2007	The Yellow Sea	Reference day		19.2	132.17
			Dust day		104.4	227.07
			Average of dust and reference			179.62

*The calculation method of the normalized flux of $N_{NH_4^+ + NO_3^-}$ was discussed in Sect. 4.4.

in some cases and lower in others. The observed ammonium in dust day samples was explained by NH_4^+ was likely either in the form of ammonium salts existing separately to dust aerosols or as the residual of incomplete reactions between ammonium salts and carbonate salts. NO_3^- in the dust day samples can be due to either mixing or reactions between anthropogenic air pollutants and dust particles or a combination of both during the transport from the source zone to the reception site. However, this process was generally much less effective and led to a sharp decrease in nitrate in TSP samples of Category 2. The existence of ammonium salt aerosols separate to dust aerosols and the extent of the reactions between ammonium salts and carbonate salts were evidently associated with the transport pathway, metrological conditions and precursor emissions and other factors. Due to a sharp increase in dust loads on dust days, the contribution of dust to the total aerosol mass increased compared to the samples collected on other days. The contributions from local anthropogenic sources were accordingly lower on dust days.

Overall, this study strongly suggested that atmospheric deposition of $N_{NH_4^+ + NO_3^-}$ on dust days varied greatly. A simple assumption of a linear increase in $N_{NH_4^+ + NO_3^-}$ with increasing dust load, like that in the literature, could lead to a considerable overestimation of the dry deposition flux of nutrients into the ocean and the consequent primary production associated with dust events.

Data availability. The data of this paper are available upon request (contact qjianhua@ouc.edu.cn).

The Supplement related to this article is available online at https://doi.org/10.5194/acp-18-571-2018-supplement.

Competing interests. The authors declare that they have no conflict of interest.

Acknowledgements. This work was supported by the Department of Science and Technology of the P. R. China through the State Key Basic Research & Development Program under grant no. 2014CB953701 and the National Natural Science Foundation of China (no. 41375143). We thank Yaqiang Wang and Jinhui Shi for the valuable discussion regarding this research. We also express our appreciation to Tianran Zhang for help with sand sampling, and Qiang Zhang, Yang Yu and Jiuren Lin for data collection.

Edited by: Barbara Ervens
Reviewed by: three anonymous referees

References

Banerjee, P. and Kumar, P. S.: Dust-induced episodic phytoplankton blooms in the Arabian Sea during winter monsoon, J. Geophys. Res.-Oceans, 119, 7123–7138, 2015.

Bielmyer, G. K., Grosell, M., and Brix, K. V.: Toxicity of silver, zinc, copper, and nickel to the copepod Acartia tonsa exposed via a phytoplankton diet, Environ. Sci. Technol., 40, 2063–2068, 2006.

Chabas, A. and Lefèvre, R. A.: Chemistry and microscopy of atmospheric particulates at Delos (Cyclades–Greece), Atmos. Environ., 34, 225–238, 2000.

Chen, D., Liu, Z., Fast, J., and Ban, J.: Simulations of sulfate–nitrate–ammonium (SNA) aerosols during the extreme haze events over northern China in October 2014, Atmos. Chem. Phys., 16, 10707–10724, https://doi.org/10.5194/acp-16-10707-2016, 2016.

CMA: Regulations of Surface Meteorological Observation, China Meteorological Press, Beijing, China, 154–156, 2004.

CMA: Sand-dust weather almanac 2008, China Meteorological Press, Beijing, China, 10–64, 2009.

CMA: Sand-dust weather almanac 2009, China Meteorological Press, Beijing, China, 11–59, 2010.

CMA: Sand-dust weather almanac 2010, China Meteorological Press, Beijing, China, 11–79, 2012.

CMA: Sand-dust weather almanac 2011, China Meteorological Press, Beijing, China, 10–53, 2013.

Creamean, J. M., Suski, K. J., Rosenfeld, D., Cazorla, A., DeMott, P. J., Sullivan, R. C., White, A. B., Ralph, F. M., Minnis, P., Comstock, J. M., Tomlinson, J. M., and Prather, K. A.: Dust and Biological Aerosols from the Sahara and Asia Influence Precipitation in the Western U.S., Science, 339, 1572–1578, 2013.

Cui, W. L.: Chemical transformation of dust components and mixing mechanisms of dust with pollution aerosols during the long range transport from north to south China, MS thesis, Department of Environmental Science and Engineering, Fudan University, China, 38 pp., 2009.

Cui, W. L., Guo, R., and Zhang, H.: The Long-range Transport of Dust from MongoliaGobi to the Yangtze River Basin and itsMixing with Pollutant Aerosols, Journal of Fudan University (Natural Science), 48, 585–592, 2009.

Dai, Y. Y.: Vertical distribution of characteristics of dust aerosols in the near-surface in hinterland of Taklimakan Desert, MS thesis, College of Resources and Environmental Science, Xinjiang University, China, 26 pp., 2016.

Dentener, F. J., Carmichael, G. R., Zhang, Y., Lelieveld, J., and Crutzen, P. J.: Role of mineral aerosol as a reactive surface in the global troposphere, J. Geophys. Res.-Atmos., 101, 22869–22889, 1996.

Duce, R. A., Liss, P. S., Merrill, J. T., Atlas, E. L., Buat-Menard, P., Hicks, B. B., Miller, J. M., Prospero, J. M., Arimoto, R., Church, T. M., Ellis, W., Galloway, J. N., Hansen, L., Jickells, T. D., Knap, A. H., Reinhardt, K. H., Schneider, B., Soudine, A., Tokos, J. J., Tsunogai, S., Wollast, R., and Zhou, M. Y.: The atmospheric input of trace species to the world ocean, Global Biogeochem. Cy., 5, 193–259, 1991.

Duce, R. A., LaRoche, J., Altieri, K., Arrigo, K. R., Baker, A. R., Capone, D. G., Cornell, S., Dentener, F., Galloway, J., Ganeshram, R. S., Geider, R. J., Jickells, T., Kuypers, M. M., Langlois, R., Liss, P. S., Liu, S. M., Middelburg, J. J., Moore, C. M., Nickovic, S., Oschlies, A., Pedersen, T., Prospero, J., Schlitzer, R., Seitzinger, S., Sorensen, L. L., Uematsu, M., Ulloa, O., Voss, M., Ward, B., and Zamora, L.: Impacts of atmospheric anthropogenic nitrogen on the open ocean, Science, 320, 893–897, 2008.

Echeveste, P., Agustí, S., and Tovar-Sánchez, A.: Toxic thresholds of cadmium and lead to oceanic phytoplankton: cell size and ocean basin-dependent effects, Environ. Toxicol. Chem., 31, 1887–1894, 2012.

Fitzgerald, E., Ault, A. P., Zauscher, M. D., Mayol-Bracero, O. L., and Prather, K. A.: Comparison of the mixing state of long-range transported Asian and African mineral dust, Atmos. Environ., 115, 19–25, 2015.

Formenti, P., Schütz, L., Balkanski, Y., Desboeufs, K., Ebert, M., Kandler, K., Petzold, A., Scheuvens, D., Weinbruch, S., and Zhang, D.: Recent progress in understanding physical and chemical properties of African and Asian mineral dust, Atmos. Chem. Phys., 11, 8231–8256, https://doi.org/10.5194/acp-11-8231-2011, 2011.

Fu, X., Wang, S. X., Cheng, Z., Xing, J., Zhao, B., Wang, J. D., and Hao, J. M.: Source, transport and impacts of a heavy dust event in the Yangtze River Delta, China, in 2011, Atmos. Chem. Phys., 14, 1239–1254, https://doi.org/10.5194/acp-14-1239-2014, 2014.

Gangwar, J. N., Gupta, T., and Agarwal, A.K.: Composition and comparative toxicity of particulate matter emitted from a diesel and biodiesel fuelled CRDI engine, Atmos. Environ., 46, 472–481, 2012.

Grice, S., Stedman, J., Kent, A., Hobson, M., Norris, J., Abbott, J., and Cooke, S.: Recent trends and projections of primary NO_2 emissions in Europe, Atmos. Environ., 43, 2154–2167, 2009.

Guo, C., Yu, J., Ho, T.-Y., Wang, L., Song, S., Kong, L., and Liu, H.: Dynamics of phytoplankton community structure in the South China Sea in response to the East Asian aerosol input, Biogeosciences, 9, 1519–1536, https://doi.org/10.5194/bg-9-1519-2012, 2012.

Han, X., Ge, C., Tao, J. H., Zhang, M. G., and Zhang, R. J.: Air quality modeling for of a strong dust event in east Asia in march 2010, Aerosol Air. Qual. Res., 12, 615–628, 2012.

Huang, K., Zhuang, G., Li, J., Wang, Q., Sun, Y., Lin, Y., and Fu, J. S.: Mixing of Asian dust with pollution aerosol and the transformation of aerosol components during the dust storm over China in spring 2007, J. Geophys. Res.-Atmos, 115, D00k13, https://doi.org/10.1029/2009jd013145, 2010.

Hwang, H. and Ro, C. U.: Direct observation of nitrate and sulfate formations from mineral dust and sea-salts using low-Z particle electron probe X-ray microanalysis, Atmos. Environ., 40, 3869–3880, 2006.

Hwang, H., Kim, H. K., and Ro, C. U.: Single-particle characterization of aerosol samples collected before and during an Asian dust storm in Chuncheon, Korea, Atmos. Environ., 42, 8738–8746, 2008.

Jickells, T. D., An, Z. S., Andersen, K. K., Baker, A. R., Bergametti, G., Brooks, N., Cao, J. J., Boyd, P. W., Duce, R. A., Hunter, K., Kawahata, H., Kubilay, N., laRoche, J.,Liss, P. S., Mahowald, N., Prospero, J. M., Ridgwell, A. J., Tegen, I., and Torres, R.: Global iron connections between desert dust, ocean biogeochemistry, and climate, Science, 308, 67–71, 2005.

Kang, E., Han, J., Lee, M., Lee, G., and Kim, J. C.: Chemical characteristics of size-resolved aerosols from Asian dust and haze episode in Seoul Metropolitan City, Atmos. Res., 127, 34–46, 2013.

Lee, Y. G., Ho, C., Kim, J., and Kim, J.: Quiescence of Asian dust events in South Korea and Japan during 2012 spring: Dust outbreaks and transports, Atmos. Environ., 114, 92–101, 2015.

Li, W. J., Shao, L. Y., Shi, Z. B., Chen, J. M., Yang, L. X., Yuan, Q., Yan, C., Zhang, X. Y., Wang, Y. Q., Sun, J. Y., Zhang, Y, M., Shen, X. J., Wang, Z. F., and Wang, W. X.: Mixing state and hygroscopicity of dust and haze particles before leaving Asian continent, J. Geophys. Res.-Atmos., 119, 1044–1059, 2014.

Lin, X. H., Liu, C. L., and Zhang, H.: Determination of Metal Elements in Aerosol by ICP-AES, Rock & Mineral Analysis, 17, 143–146, 1998.

Liu, L., Zhang, X., Xu, W., Liu, X., Li, Y., Lu, X., Zhang, Y., and Zhang, W.: Temporal characteristics of atmospheric ammonia and nitrogen dioxide over China based on emission data, satellite observations and atmospheric transport modeling since 1980, Atmos. Chem. Phys., 17, 9365–9378, https://doi.org/10.5194/acp-17-9365-2017, 2017.

Liu, Q. Y. and Bei, Y. L.: Impacts of crystal metal on secondary aliphatic amine aerosol formation during dust storm episodes in Beijing, Atmos. Environ., 128, 227–234, 2016.

Liu, Q. Y., Liu, Y. J., Yin, J. X., Zhang, M. G., and Zhang, T. T.: Chemical characteristics and source apportionment of PM_{10} during Asian dust storm and non-dust storm days in Beijing, Atmos. Environ., 91, 85–94, 2014.

Liu, X. H., Zhang, Y., Cheng, S. H., Xing, J., Zhang, Q., Streets, D. G., Jang, C., Wang, W. X., and Hao, J. M.: Understanding of regional air pollution over China using CMAQ, part I performance evaluation and seasonal variation, Atmos. Environ., 44, 2415–2426, 2010a.

Liu, X. H., Zhang, Y., Xing, J., Zhang, Q., Wang, K., Streets, D. G., Jang, C., Wang, W. X., and Hao, J. M.: Understanding of regional air pollution over China using CMAQ, part II. Process analysis and sensitivity of ozone and particulate matter to precursor emissions, Atmos. Environ., 44, 3719–3727, 2010b.

Liu, Y., Zhang, T. R., Shi, J. H., Gao, H. W., and Yao, X. H.: Responses of chlorophyll a to added nutrients, Asian dust, and rainwater in an oligotrophic zone of the Yellow Sea: Implications for promotion and inhibition effects in an incubation experiment, J. Geophys. Res.-Biogeo., 118, 1763–1772, 2013.

Ma, Q. X., Liu, Y. C., Liu, C., Ma, J. Z., and He, H.: A case study of Asian dust storm particles: Chemical composition, reactivity to SO_2 and hygroscopic properties, J. Environ. Sci., 24, 62–71, 2012.

Mori, I., Nishikawa, M., Tanimura, T., and Quan, H.: Change in size distribution and chemical composition of kosa (Asian dust) aerosol during long-range transport, Atmos. Environ., 37, 4253–4263, 2003.

Niu, S. J. and Zhang, C. C.: Researches on sand aerosol chemical composition and enrichment factor in the spring at Helan Mountain area, J. Desert Res., 20, 264–268, 2000.

Ohara, T., Akimoto, H., Kurokawa, J., Horii, N., Yamaji, K., Yan, X., and Hayasaka, T.: An Asian emission inventory of anthropogenic emission sources for the period 1980–2020, Atmos. Chem. Phys., 7, 4419–4444, https://doi.org/10.5194/acp-7-4419-2007, 2007.

Paatero, P.: Least squares formulation of robust non-negative factor analysis, Chemometr. Intell. Lab., 37, 23–35, 1997.

Paatero, P. and Tapper, U.: Analysis of different modes of factor analysis as least squares fit problems, Chemometr. Intell. Lab., 18, 183–194, 1993.

Penrod, A., Zhang, Y., Wang, K., Wu, S. Y., and Leung, L. R.: Impacts of future climate and emission changes on U.S. air quality, Atmos. Environ., 89, 533–547, 2014.

Qi, J. H., Li, P. L., Li, X. G., Feng, L. J., and Zhang, M. P.: Estimation of dry deposition fluxes of particulate species to the water surface in the Qingdao area, using a model and surrogate surfaces, Atmos. Environ., 39, 2081–2088, 2005.

Qi, J. H., Gao, H. W., Yu, L. M., and Qiao, J. J.: Distribution of inorganic nitrogen-containing species in atmospheric particles from an island in the Yellow Sea, Atmos. Res., 101, 938–955, 2011.

Qi, J. H., Shi, J. H., Gao, H. W., and Sun, Z.: Atmospheric dry and wet deposition of nitrogen species and its implication for primary productivity in coastal region of the Yellow Sea, China, Atmos. Environ., 81, 600–608, 2013.

Scheinhardt, S., Müller, K., Spindler, G., and Herrmann, H.: Complexation of trace metals in size-segregated aerosol particles at nine sites in Germany, Atmos. Environ., 74, 102–109, 2013.

Seinfeld, J. H. and Pandis, S. N.: Atmospheric Chemistry and Physics: From Air Pollution to Climate Change, 2nd Edition, Wiley, New York, USA, 1191 pp., 1998.

Sheng, Y., Yang, S., Han, Y., Zheng, Q., and Fang, X.: The concentrations and sources of nitrate in aerosol over Dolmud, Qinghai, China, J. Desert Res., 36, 792–797, 2016.

Shi, J. H., Gao, H. W., Zhang, J., Tan, S. C., Ren, J. L., Liu, C. G., Liu, Y., and Yao, X. H.: Examination of causative link between a spring bloom and dry/wet deposition of Asian dust in the Yellow Sea, China, J. Geophys. Res.-Atmos., 117, 127–135, 2012.

Shi, J. H., Zhang, J., Gao, H. W., Tan, S. C., Yao, X. H., and Ren, J. L.: Concentration, solubility and deposition flux of atmospheric particulate nutrients over the Yellow Sea, Deep-Sea Res. Pt. II, 97, 43–50, 2013.

Skjøth, C. A. and Hertel, O.: Ammonia Emissions in Europe, in Urban Air Quality in Europe, Springer Berlin Heidelberg, Germany, 141–164, 2013.

Sobanska, S., Hwang, H., Choël, M., Jung, H., Eom, H., Kim, H., Barbillat, J., and Ro C.: Investigation of the Chemical Mixing State of Individual Asian Dust Particles by the Combined Use of Electron Probe X-ray Microanalysis and Raman Microspectrometry, Anal. Chem., 84, 3145–3154, 2012.

Su, X., Wang, Q., Li, Z., Calvello, M., Esposito, F., Pavese, G., Lin, M., Cao, J., Zhou, C., Li, D., and Xu, H.: Regional transport of anthropogenic pollution and dust aerosols in spring to Tianjin – A coastal megacity in China, Sci. Total. Environ., 584–585, 381–392, 2017.

Tan, S. C. and Wang, H.: The transport and deposition of dust and its impact on phytoplankton growth in the Yellow Sea, Atmos. Environ., 99, 491–499, 2014.

Taylor, S. R.: Abundance of chemical elements in the continental crust: a new table, Geochim. Cosmochim. Ac., 28, 1273–1285, 1964.

Tobo, Y., Zhang, D. Z., Matsuki, A., and Iwasaka, Y.: Asian dust particles converted into aqueous droplets under remote marine atmospheric conditions, P. Natl. Acad. Sci. USA, 107, 17905–17910, 2010.

Underwood, G. M., Song, C. H., Phadnis, M., Carmichael, G. R., and Grassian, V. H.: Heterogeneous reactions of NO_2 and HNO_3 on oxides and mineral dust: a combined laboratory and modeling study, J. Geophys. Res.-Atmos., 106, 18055–18066, 2001.

Uno, I., Eguchi, K., Yumimoto, K., Takemura, T., Shimizu, A., Uematsu, M., Liu, Z., Wang, Z., Hara, Y., and Sugimoto, N.: Asian dust transported one full circuit around the globe, Nat. Geosci., 2, 557–560, 2009.

U.S. EPA: Method 1631, Revision E: Mercury in water by oxidation, purge and trap, and cold vapor atomic fluorescence spectrometry, US Environmental Protection Agency, Washington, D.C., USA, 2002.

Van Curen, R. and Cahill, T.: Asian aerosols in North America: Frequency and concentration of fine dust, J. Geophys. Res., 107, 4804, https://doi.org/10.1029/2002JD002204, 2002.

Walker, J. M., Philip, S., Martin, R. V., and Seinfeld, J. H.: Simulation of nitrate, sulfate, and ammonium aerosols over the United States, Atmos. Chem. Phys., 12, 11213–11227, https://doi.org/10.5194/acp-12-11213-2012, 2012.

Wang, F. J., Chen, Y., Guo, Z. G., Gao, H. W., Mackey, K. R., Yao, X. H., Zhuang, G. S., and Paytan, A.: Combined effects of iron and copper from atmospheric dry deposition on ocean productivity, Geophys. Res. Lett., 44, 2546–2555, 2017.

Wang, H., An, J., Shen, L., Zhu, B., Xia, L., Duan, Q., and Zou, J.: Mixing state of ambient aerosols in Nanjing city by single particle mass spectrometry, Atmos. Environ., 132, 123–132, 2016.

Wang, L., Du, H. H., Chen, J. M., Zhang, M., Huang, X. Y., Tan, H. B., Kong, L. D., and Geng, F. H.: Consecutive transport of anthropogenic air masses and dust storm plume: Two case events at Shanghai, China, Atmos. Res., 127, 22–33, 2013.

Wang, Q. Z., Zhuang, G. S., Li, J., Huang, K., Zhang, R., Jiang, Y. L., Lin, Y. F., and Fu, J. S.: Mixing of dust with pollution on the transport path of Asian dust - Revealed from the aerosol over Yulin, the north edge of Loess Plateau, Sci. Total. Environ., 409, 573–581, 2011.

Wang, Q. Z., Zhuang, G. S., Huang, K., Liu, T. N., Lin, Y. F., Deng, C. R., Fu, Q. Y., Fu, J. S., Chen, J. K., Zhang, W. J., and Yiming, M.: Evolution of particulate sulfate and nitrate along the Asian dust pathway: Secondary transformation and primary pollutants via long-range transport, Atmos. Res., 169, 86–95, 2016.

Wang, Y. Q., Zhang, X. Y., Gong, S. L., Zhou, C. H., Hu, X. Q., Liu, H. L., Niu, T., and Yang, Y. Q.: Surface observation of sand and dust storm in East Asia and its application in CUACE/Dust, Atmos. Chem. Phys., 8, 545–553, https://doi.org/10.5194/acp-8-545-2008, 2008.

Wang, Y. Q., Zhang, X. Y., and Draxler, R. R.: TrajStat: GIS-based software that uses various trajectory statistical analysis methods to identify potential sources from long-term air pollution measurement data, Environ. Modell. Softw., 24, 938–939, 2009.

Wang, Z., Pan, X., Uno, I., Li, J., Wang, Z., Chen, X., Fu, P., Yang, T., Kobayashi, H., Shimizu, A., Sugimoto, N., and Yamamoto, S.: Significant impacts of heterogeneous reactions on the chemical composition and mixing state of dust particles: A case study during dust events over northern China, Atmos. Environ., 159, 83–91, 2017.

Williams, R. W.: A model for the dry deposition of particles to natural water surface, Atmos. Environ., 16, 1933–1938, 1982.

Wu, F., Zhang, D., Cao, J., Guo, X., Xia, Y., Zhang, T., Lu, H., and Cheng, Y.: Limited production of sulfate and nitrate on front-associated dust storm particles moving from desert to distant populated areas in northwestern China, Atmos. Chem. Phys., 17, 14473–14484, https://doi.org/10.5194/acp-17-14473-2017, 2017.

Xie, R. K., Seip, H. M., Leinum, J. R., Winje, T., and Xiao, J. S.: Chemical characterization of, individual particles (PM_{10}) from ambient air in Guiyang City, Sci. Total. Environ., 343, 261–271, 2005.

Xin, W. C., Lin, X. H., and Xu, L.: ICP-MS Determination of 34 trace elements in marine sediments, Phys. Test. Chem. Anal. B, 48, 459–464, 2012.

Xu, J. Z., Wang, Z. B., Yu, G. M., Qin, X., Ren, J. W., and Qin, D. H.: Characteristics of water soluble ionic species in fine particles from a high altitude site on the northern boundary of Tibetan Plateau: Mixture of mineral dust and anthropogenic aerosol, Atmos. Res., 143, 43–56, 2014.

Yang, D. Z., Wang, C., Wen, Y. P., Yu, X. L., and Xiu, X. B.: Analysis of Two Sand Storms In Spring 1990, Q. J. Appl. Meteorol., 6, 18–26, 1995.

Yang, D. Z., Yan, P., and Xu, X. D.: Characteristics of aerosols under dust and sand weather in Beijing, Q. J. Appl. Meteorol., 1, 185–194, 2002.

Yao, X. H. and Zhang, L.: Supermicron modes of ammonium ions related to fog in rural atmosphere, Atmos. Chem. Phys., 12, 11165–11178, https://doi.org/10.5194/acp-12-11165-2012, 2012.

Yao, X. H., Lau, A. S., Fang, M., Chan, C., and Hu, M.: Size Distributions and Formation of Ionic Species in Atmospheric Particulate Pollutants in Beijing, China: 1 – Inorganic Ions, Atmos. Environ., 37, 2991–3000, 2003.

Zhang, G., Han, B., Bi, X., Dai, S., Huang, W., Chen, D., Wang, X., Sheng, G., Fu, J., and Zhou, Z.: Characteristics of individual particles in the atmosphere of Guangzhou by single particle mass spectrometry, Atmos. Res., 153, 286–295, 2015.

Zhang, G. S., Zhang, J., and Liu, S. M.: Characterization of nutrients in the atmospheric wet and dry deposition observed at the two monitoring sites over Yellow Sea and East China Sea, J. Atmos. Chem., 57, 42–57, 2007.

Zhang, J., Zhang, G. S., Bi, Y. F., and Liu, S. M.: Nitrogen species in rainwater and aerosols of the Yellow and East China seas: Effects of the East Asian monsoon and anthropogenic emissions and relevance for the NW Pacific Ocean, Global Biogeochem. Cy., 25, 113–120, 2011.

Zhang, K. and Gao, H. W.: The characteristics of Asian-dust storms during 2000–2002: From the source to the sea, Atmos. Environ., 41, 9136–9145, 2007.

Zhang, Q., Streets, D. G., Carmichael, G. R., He, K. B., Huo, H., Kannari, A., Klimont, Z., Park, I. S., Reddy, S., Fu, J. S., Chen, D., Duan, L., Lei, Y., Wang, L. T., and Yao, Z. L.: Asian emissions in 2006 for the NASA INTEX-B mission, Atmos. Chem. Phys., 9, 5131–5153, https://doi.org/10.5194/acp-9-5131-2009, 2009.

Zhang, W. J., Zhuang, G. S., Huang, K., Li, J., Zhang, R., Wang, Q. Z., Sun, Y. L., Fu, J. S., Chen, Y., and Xu, D. Q.: Mixing and transformation of Asian dust with pollution in the two dust storms over the northern China in 2006, Atmos. Environ., 44, 3394–3403, 2010.

Zhang, Y. and Carmichael, G. R.: The role of mineral aerosol in tropospheric chemistry in East Asia – a model study, J. Appl. Meteorol., 38, 353–366, 1999.

Zhang, Y., Sunwoo, Y., Kotamarthi, V. R., and Carmichael, G. R.: Photochemical oxidant processes in the presence of dust: an evaluation of the impact of dust on particulate nitrate and ozone formation, J. Appl. Meteorol., 33, 813–824, 1994.

Zhang, Y., Yu, Q., Ma, W. C., and Chen, L. M.: Atmospheric deposition of inorganic nitrogen to the eastern China seas and its implications to marine biogeochemistry, J. Geophys. Res.-Atmos., 115, D00K10, https://doi.org/10.1029/2009JD012814, 2010.